
LABORATORY INVESTIGATION

Optical Quality of the Eye Degraded by Time-Varying Wavefront Aberrations with Tear Film Dynamics

Yoko Hirohara^{1,3}, Toshifumi Mihashi^{1,3}, Shizuka Koh², Sayuri Ninomiya¹,
Naoyuki Maeda², and Takashi Fujikado¹

¹Department of Applied Visual Science, Osaka University Graduate School of Medicine, Osaka, Japan; ²Department of Ophthalmology, Osaka University Graduate School of Medicine, Osaka, Japan; ³Research Institute, Topcon Corporation, Tokyo, Japan

Abstract

Purpose: Wavefront aberrations (WFAs) of the eye vary with time because of the tear film dynamics. We investigated, using a simulation method, the variation of optical quality with time-varying wavefront measurements of 13 eyes with different refractions.

Methods: WFAs of 13 normal eyes of 13 subjects were measured every second for 10 s. First, we simulated WFAs with conventional corneal laser refractive surgery by subtracting the second-order aberrations of the least aberrated measurement from measured consecutive WFAs. Second, we simulated customized refractive surgery by subtracting the second- to sixth-order aberrations of the least aberrated measurement from measured consecutive WFAs. We calculated Strehl ratios and retinal images from these corrected consecutive WFAs.

Results: In one eye, the root mean square (RMS) values of WFAs with a second-order correction were sometimes smaller than those of WFAs with a second- to sixth-order correction, when these were compared at the same time point after a blink. However, in the other 12 eyes, the RMS values with second- to sixth-order corrections were smaller than those with only a second-order correction. In eight eyes, the Strehl ratios with second- to sixth-order corrections were larger than those with second-order corrections. In the remaining five eyes, Strehl ratios with second- to sixth-order corrections were sometimes smaller than those with second-order corrections.

Conclusions: In a simulation, the correction of time-invariant higher order aberrations usually reduced RMS values, but it did not always result in higher Strehl ratios than those obtained with only second-order corrections. **Jpn J Ophthalmol** 2007;51:258–264 © Japanese Ophthalmological Society 2007

Key Words: aberration, retinal image, Shack-Hartmann aberrometer, Strehl ratio, tear film

Introduction

Studies of wavefront aberrations (WFAs) of human eyes have clearly revealed that the optical quality of the eyes is degraded by monochromatic aberrations.^{1,2} This degradation is caused not only by static phenomena but also by

ocular dynamics.^{3,4} The typical ocular dynamics involved in degrading optical quality are tear film dynamics,^{5–7} ocular accommodation,^{8,9} and cardiovascular activity.¹⁰

Tear film dynamics have been studied by consecutive measurements of the cornea with a Placido's disk videokeratoscope.^{11–14} Nemeth et al.¹¹ measured changes in the surface regularity index, the surface asymmetry index, and corneal power. Goto et al.¹² and Kojima et al.¹³ calculated changes in the break-up area and break-up time from Placido's disk images. Montes-Mico et al.¹⁴ evaluated corneal WFAs calculated from Placido's disk images for dry eye patients. Recently, post-blink aberration changes were

Received: July 18, 2006 / Accepted: March 1, 2007

Correspondence and reprint requests to: Takashi Fujikado, Department of Applied Visual Science, Osaka University Graduate School of Medicine, Room G4, 2-2 Yamadaoka, Suita, Osaka 565-0871, Japan
e-mail: fujikado@ophthal.med.osaka-u.ac.jp

investigated by measuring point-spread functions (PSF)⁵ and ocular WFAs.^{6,7} Ocular WFAs increase several seconds after a blink.⁵⁻⁷ Tutt et al.¹⁵ studied optical quality related to tear film dynamics.

To investigate the changes in optical quality with tear film dynamics, we measured post-blink WFAs consecutively. We then employed simple computational models, as described below, to simulate WFAs for eyes that had undergone conventional corneal laser refractive surgery or refractive correction with spectacles, as well as for eyes that had undergone customized corneal laser refractive surgery or refractive correction with customized contact lenses. We simulated time variations of the PSF, Strehl ratio, and the retinal images of Landolt's rings from these computed consecutive WFAs.

Methods

The WFAs were measured in 13 normal eyes of 13 subjects, average age, 29.5 ± 4.2 years. The average \pm SD of spherical error for the 13 eyes was -2.50 ± 3.28 , and the average \pm SD of break-up time was 7.31 ± 1.80 . Written informed consent was obtained from each subject. The procedures were performed to conform to the tenets of the Declaration of Helsinki. WFAs were measured using a prototype Shack-Hartmann wavefront aberrometer (Topcon, Tokyo, Japan) once every second for 10s, immediately after blinking. Lenslet size was 0.22mm^2 on the pupil plane, and the focal length was 5mm. WFAs were analyzed using normalized Zernike polynomials defined over a 4-mm-diameter area in the center of the pupil. The coefficients up to the sixth order were calculated.

We simulated two types of refractive corrections: second-order correction and second- to sixth-order correction. Figure 1 shows the method of these corrections.

WFAs are expressed by the following equation:

$$W(x, y, t) = \sum_{i=2}^6 \sum_{j=0}^i c_i^{-i+2j}(t) z_i^{-i+2j}(x, y), \quad (1)$$

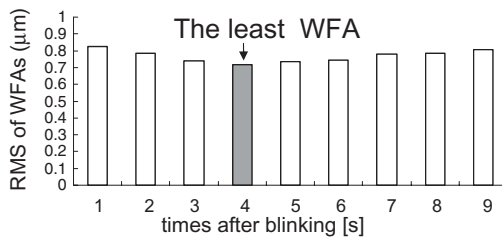
where $W(x, y, t)$ is a WFA, x and y are horizontal and vertical coordinates on the pupil, t is the time after blink, $c_i(t)$ is the Zernike coefficient, and $z_i(x, y)$ is the Zernike polynomial. The tilt terms were omitted because they did not affect the visual effect. The least aberrated wavefront measurement that had the smallest root mean square (RMS) value of WFAs for the measurements in each trial was chosen for the simulation. This minimal wavefront was chosen to represent the time-invariant, potentially correctable component of the total aberration. Depending upon the type of correction, either only the second-order terms or all of the terms of this wavefront were subtracted from all of the measured wavefronts in the time series to simulate the correction.

The WFAs that had the smallest RMS value of measured WFAs in each trial are described by

$$W(x, y, t_{\min}) = \sum_{i=2}^6 \sum_{j=0}^i c_i^{-i+2j}(t_{\min}) z_i^{-i+2j}(x, y), \quad (2)$$

where t_{\min} is the time after blink when the RMS value of the WFA becomes the smallest.

In the second-order correction, retinal images were simulated by using WFAs for which only the second-order aberrations were corrected. The second-order corrected WFA, $W_{2nd_co}(x, y, t)$, is expressed by the following equation:



simulation of
second-order
correction

simulation of
second- to sixth-
order correction

Subtract only second-order
coefficients of the least WFAs
from the WFA coefficients of
each time point.

Subtract the second- to sixth-
order coefficients of the least
WFAs from the WFA
coefficients of each time point.

Simulation

Simulation

Figure 1. Methods of second-order correction and second- to sixth-order correction. WFA, wavefront aberrations.

$$\begin{aligned}
W_{2nd_co}(x, y, t) &= \sum_{i=2}^6 \sum_{j=0}^i c_i^{-i+2j}(t) z_i^{-i+2j}(x, y) \\
&\quad - \sum_{j=0}^2 c_2^{-2+2j}(t_{\min}) z_2^{-2+2j}(x, y) \\
&= \sum_{j=0}^2 \{c_2^{-2+2j}(t) - c_2^{-2+2j}(t_{\min})\} z_2^{-2+2j}(x, y) \\
&\quad + \sum_{i=3}^6 \sum_{j=0}^i c_i^{-i+2j}(t) z_i^{-i+2j}(x, y). \tag{3}
\end{aligned}$$

The second- to sixth-order correction was simulated by subtracting the second- to sixth-order aberrations of the $W(x, y, t_{\min})$ from each WFA. The second- to sixth-order corrected WFA $W_{2nd_6th_co}(x, y, t)$ is expressed by the following equation:

$$\begin{aligned}
W_{2nd_6th_co}(x, y, t) &= \sum_{i=2}^6 \sum_{j=0}^i c_i^{-i+2j}(t) z_i^{-i+2j}(x, y) \\
&\quad - \sum_{i=2}^6 \sum_{j=0}^i c_i^{-i+2j}(t_{\min}) z_i^{-i+2j}(x, y) \\
&= \sum_{i=2}^6 \sum_{j=0}^i \{c_i^{-i+2j}(t) - c_i^{-i+2j}(t_{\min})\} z_i^{-i+2j}(x, y). \tag{4}
\end{aligned}$$

It is clear that $W_{2nd_6th_co}(x, y, t)$ becomes zero when $t = t_{\min}$.

The series of residual RMS values for each WFA, PSF, Strehl ratio, and retinal image of the Landolt's rings after second-order correction and after second- to sixth-order correction were simulated.

The PSF was calculated from the pupil function by a fast Fourier transform (FFT). When we constructed the pupil function, we used the second-order corrected WFA and second- to sixth-order corrected WFA. Then the optical transfer function (OTF) was calculated from the PSF by again using FFT. The Strehl ratio was calculated in the process of calculating the OTF.¹⁶ We compared the Strehl ratio and the RMS of measured WFAs.

Results

The results for two eyes of two subjects, HT (24 years old) and YH (29 years old), are shown in Figs. 2 and 3. The RMS of measured WFAs became a minimum at 2 s after blinking for HT and 4 s after blinking for YH.

The RMS values of the W_{2nd_co} ranged from 0.065 to 0.337 μm for HT and from 0.068 to 0.266 μm for YH. RMS values of the $W_{2nd_6th_co}$ ranged from 0 to 0.204 μm for HT and from 0 to 0.153 μm for YH.

The minimum Strehl ratios calculated from W_{2nd_co} and $W_{2nd_6th_co}$ were 0.066 and 0.102, respectively, for HT. The Strehl ratio calculated from $W_{2nd_6th_co}$ was always larger than that calculated from W_{2nd_co} . With the minimum Strehl ratio, simulated Landolt's rings of $W_{2nd_6th_co}$ were clearer than those of W_{2nd_co} for HT.

The minimum Strehl ratios calculated from W_{2nd_co} and from $W_{2nd_6th_co}$ were 0.129 and 0.105 for YH. The Strehl

ratios calculated from $W_{2nd_6th_co}$ were sometimes smaller than those calculated from W_{2nd_co} . When the Strehl ratio calculated from $W_{2nd_6th_co}$ was smaller than that calculated from W_{2nd_co} , the Landolt's rings calculated from $W_{2nd_6th_co}$ were more blurred than those calculated from W_{2nd_co} . It was more difficult to recognize the gap in the simulated 20/20 Landolt's rings of $W_{2nd_6th_co}$ than the gap in the rings of W_{2nd_co} .

Figure 4 shows graphs of the RMS values of W_{2nd_co} and of $W_{2nd_6th_co}$ in the 13 normal eyes of 13 subjects. For 12 of the 13 eyes, the RMS values of the W_{2nd_co} were larger than those of the $W_{2nd_6th_co}$ in one series of measurements. One of the 13 eyes had RMS values of W_{2nd_co} that were occasionally smaller than those of $W_{2nd_6th_co}$ (Fig. 4, arrow).

Figure 5 shows graphs of Strehl ratios calculated from W_{2nd_co} and $W_{2nd_6th_co}$ of the 13 normal eyes of the 13 subjects. For five of those 13 eyes, the Strehl ratios with the W_{2nd_co} were larger than those with the $W_{2nd_6th_co}$ in one series of measurements (Fig. 5, arrows). Three of these five eyes had this inverse relationship just after blinking. One of the eyes had the inverse relationship between 3 and 7 s after blinking. The other eye had the inverse relationship 8 s after blinking, which was the last measurement of the time course.

The Strehl ratio and RMS of $W_{2nd_6th_co}$ were significantly correlated for all 13 eyes (Pearson's correlation coefficient, $P < 0.01$), and the Strehl ratio and RMS of W_{2nd_co} were correlated for 10 of the 13 eyes (Pearson's correlation coefficient, $P < 0.05$).

Discussion

The average RMS values of the time-varying $W_{2nd_6th_co}$ for a 4-mm pupil was 0.204 μm for HT and 0.153 μm for YH. Considering that the average RMS for the normal population is 0.08 μm ,¹⁷ these residual aberrations are large.

In most cases, the RMS values of the $W_{2nd_6th_co}$ were smaller than those of the W_{2nd_co} . However, one of the 13 eyes had RMS values of the W_{2nd_co} that were occasionally smaller than those of the $W_{2nd_6th_co}$. This could happen when the higher order aberrations varied greatly from those for the minimum aberration that we used for the correction.

The Strehl ratio of W_{2nd_co} was once larger than that of $W_{2nd_6th_co}$ for YH. This did not happen for HT. Five of the 13 eyes we measured had the same results. The Strehl ratio I is expressed as

$$\begin{aligned}
I &= \frac{1}{\pi^2} \left| \int_0^1 \int_0^{2\pi} e^{i \frac{2\pi}{\lambda} W} \rho d\rho d\theta \right|^2 \\
&= \frac{1}{\pi^2} \left| \int_0^1 \int_0^{2\pi} \left[1 + i \frac{2\pi}{\lambda} W + \frac{1}{2} \left(i \frac{2\pi}{\lambda} W \right)^2 + \dots \right] \rho d\rho d\theta \right|^2, \tag{5}
\end{aligned}$$

where W is the wavefront aberration, ρ and θ are the radius and azimuth in the polar coordinate system. If we assume that the wavefront aberrations are so small that we may

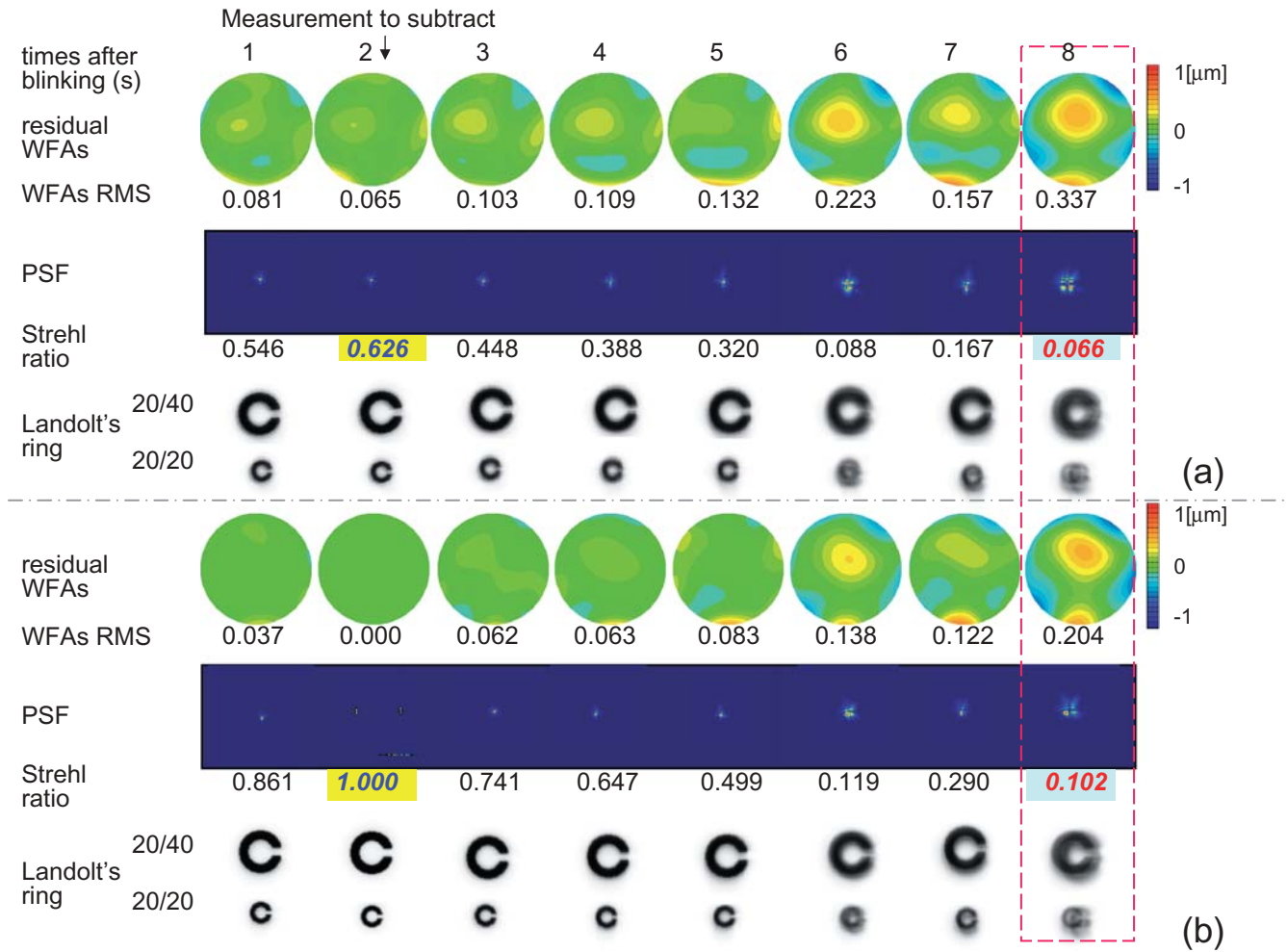


Figure 2a, b. Simulation results for subject HT. **a** Second-order correction. **b** Second- to sixth-order correction. The first row shows time after blinking (s), and the following row depicts color-coded maps of residual WFAs. RMS, root mean square; PSF, point-spread function. Strehl ratio. Simulated Landolt's ring images of targets for visual acuity of 20/40 and 20/20. The blue numbers in the yellow ground are maximum Strehl ratios, and the red numbers in the light blue ground are minimum Strehl ratios in the series. At top of figure, the *arrow* indicates the measurement to subtract.

neglect the third- and higher orders of wavefront aberrations in (5), then I is expressed as

$$I \approx 1 - \left(\frac{2\pi}{\lambda}\right)^2 \left[\overline{W^2} - (\overline{W})^2\right]. \quad (6)$$

The second term of the right-hand side of the equation represents the RMS. The larger the RMS is, the smaller the Strehl ratio is. However, this is not true when the higher order terms of equation (5) are included in the calculation of the Strehl ratio. Applegate et al.¹⁹ reported that the impact on the retinal image of different aberration terms differs; some combinations of aberration terms even increase visual performance, although those combinations also increase the RMS error. Oshika et al.²⁰ showed that the aberrated eye can show apparent accommodation. Cheng et al.²¹ reported that spherical aberration, coma, and secondary astigmatism all reduce visual acuity and increase depth of focus. Both reported that some higher order aber-

rations combined with specific low-order aberrations can improve, instead of reduce, image quality. We therefore cannot determine all of the effects of aberrations on visual function from the RMS alone.

This 10-s measurement duration is longer than the usual blink interval, which is around 4 to 5 s.²² This longer duration could increase aberrations and degrade images because of tear film break-up. Nine of the 13 eyes had smaller Strehl ratios at the last measurement than at the first measurement (on average for 4 s just after blinking). The tear film conditions in the other eyes were not considered to be influenced by the longer duration.

Three eyes had smaller Strehl ratios with the $W_{2nd_6th_co}$ than with the W_{2nd_co} just after blinking. The Strehl ratios were the smallest or the second smallest toward the end of the 10-s interval. The small Strehl ratio just after blinking was most likely due to the inhomogeneous tear film caused by the blink. Neuronal visual function is suppressed just

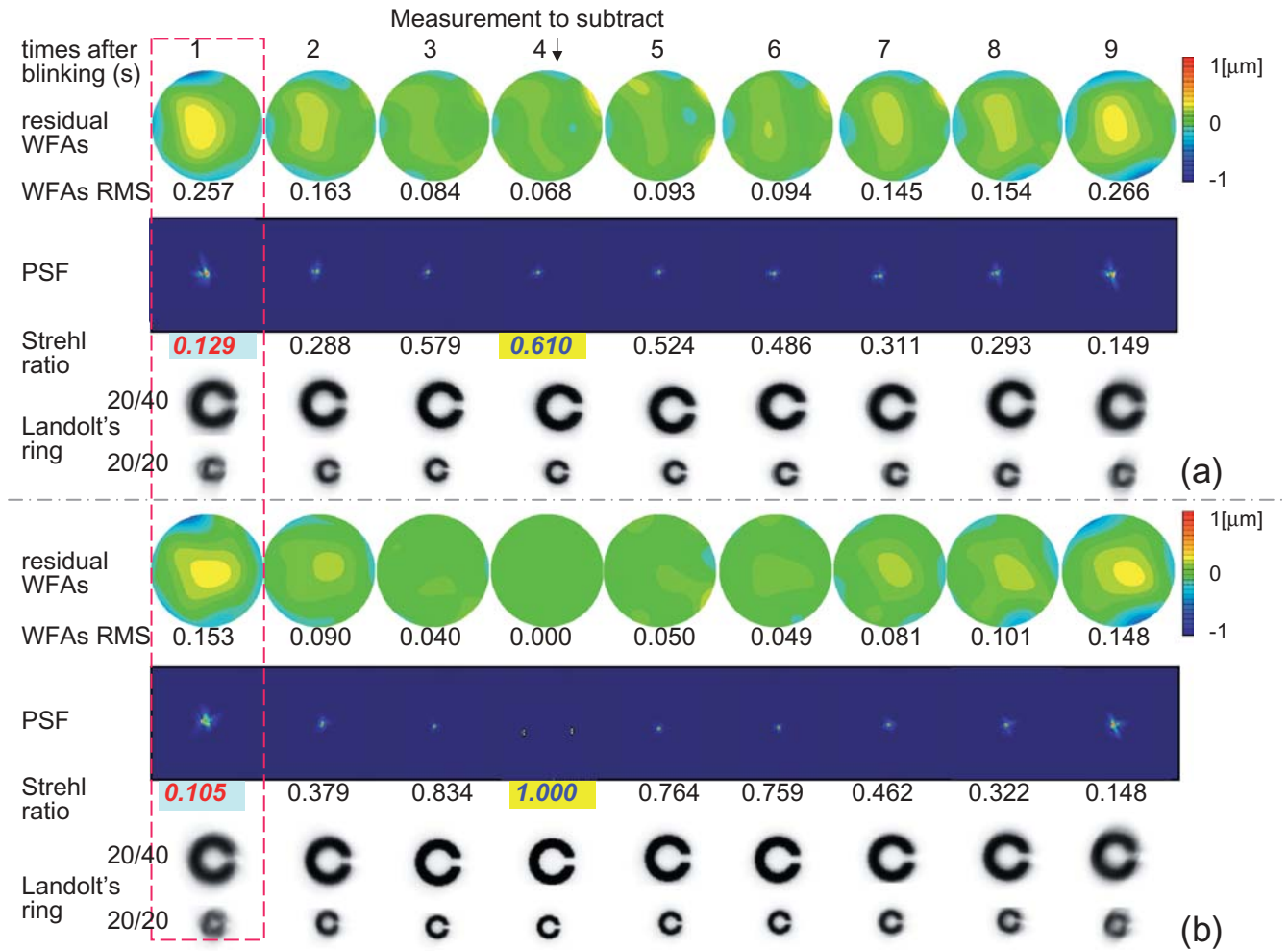


Figure 3a, b. Simulation results for subject YH. **a** Second-order correction. **b** Second- to sixth-order correction. See legend of Fig. 2 for other details.

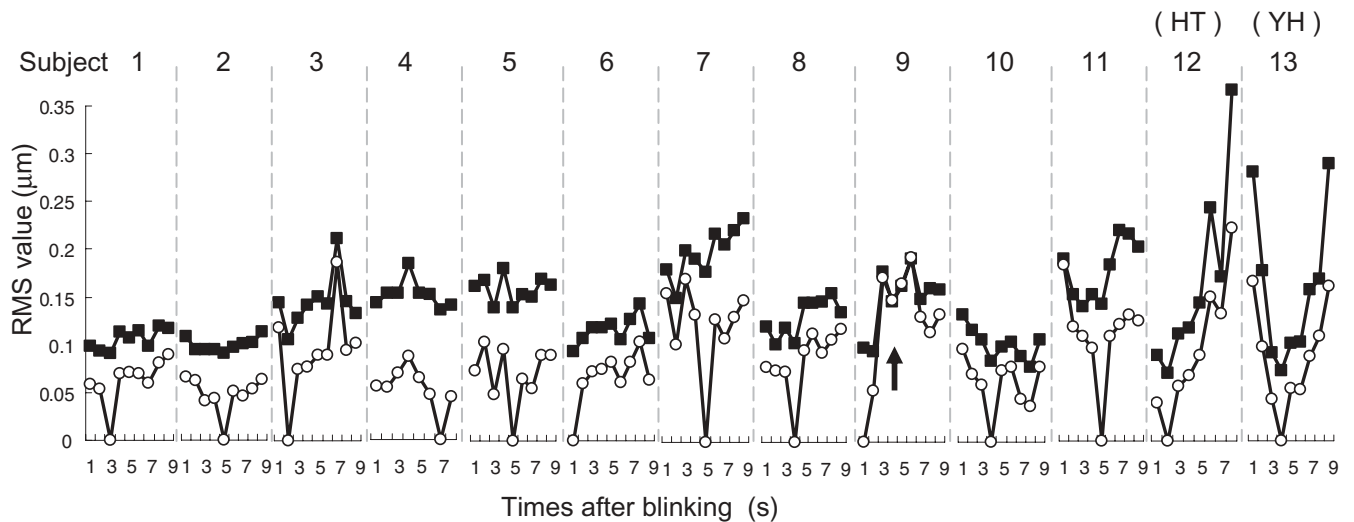


Figure 4. Graphs of RMS values after second-order correction and second- to sixth-order correction in 13 normal eyes of 13 subjects. —■— simulation of second-order correction. —○— simulation of second- to sixth-order correction.

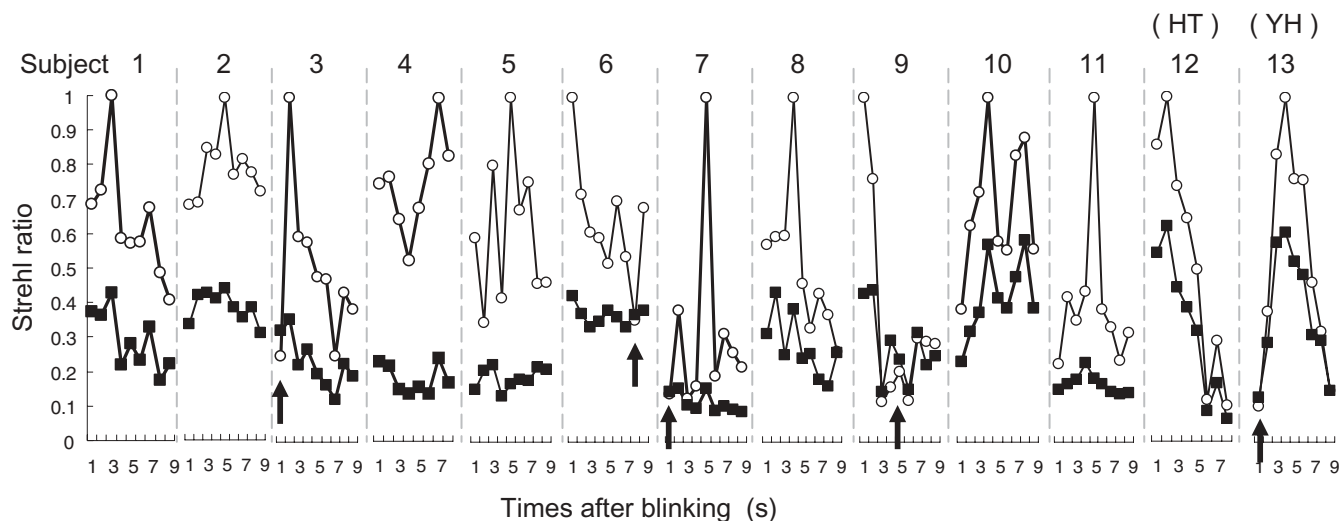


Figure 5. Graphs of Strehl ratios after second-order correction and second- to sixth-order correction of 13 normal eyes of 13 subjects. —■— simulation of second-order correction. —○— simulation of second- to sixth-order correction.

after blinking,²³ and this suppression may help to prevent the transfer of bad retinal images to the brain.

In this research, we found that RMS error was always more reduced after correction of the second- to sixth-order aberrations than after correction of only second-order aberrations, but image quality was sometimes not improved more by the former than by the latter. When customized corneal refractive surgery is performed, it should be taken into account that the aberrations of the eye fluctuate. It may be preferable to measure aberrations several times and correct only those aberrations that are significantly larger than the fluctuations in measurements.

In the simulation, we assumed that aberrations of the eye can be corrected perfectly. However, it has been reported that higher order aberrations after customized refractive surgery are almost the same or increased.^{24–27} Therefore, the simulations differed from the results of recent customized refractive surgery. We are not certain that it will be possible to develop a perfect corneal customized refractive surgery to correct all aberrations in the future.

Thai et al.²⁸ measured contrast sensitivity before pre-contact lens tear break-up by a stimulus presented 2s after the blink. Measurements of visual performance and tear break-up using a tear scope were made simultaneously in this experiment. It was found that contrast sensitivity is reduced after the pre-lens tear film break-up, and this effect is increased with higher spatial frequencies.²⁸ Ishida et al.²⁹ measured monocular recognition acuity continuously during a 30-s blink-free period using continuous functional visual acuity measurement (FVAM), and they found that the mean FVAM results sometimes decreased during testing in both dry eye patients and control subjects.²⁹ Because we found that Strehl ratios and retinal images fluctuated from tear film conditions in this study, we are planning to compare these data with subjective data in the future.

Acknowledgment. The authors thank Prof. Howard Howland (Cornell University) for his helpful comments on the manuscript.

References

- Porter J, Guirao A, Cox IG, Williams DR. Monochromatic aberrations of the human eye in a large population. *J Opt Soc Am A Opt Image Sci Vis* 2001;18:1793–1803.
- Thibos LN, Hong X, Bradley A, Cheng X. Statistical variation of aberration structure and image quality in a normal population of healthy eyes. *J Opt Soc Am A Opt Image Sci Vis* 2002;19:2329–2348.
- Hofer H, Artal P, Singer B, Aragon JL, Williams DR. Dynamics of the eye's wave aberration. *J Opt Soc Am A Opt Image Sci Vis* 2001;18:497–506.
- Diaz-Santana L, Torti C, Munro I, Gasson P, Dainty C. Benefit of higher closed-loop bandwidths in ocular adaptive optics. *Opt Express* 2003;11:2597–2605.
- Montes-Mico R, Alio JL, Charman WN. Postblink changes in the ocular modulation transfer function measured by a double-pass method. *Invest Ophthalmol Vis Sci* 2005;46:4468–4473.
- Mihashi T, Hirohara Y, Koh S, Ninomiya S, Maeda N, Fujikado T. Tear film break-up time evaluated by real-time Hartmann-Shack wavefront sensing. *Jpn J Ophthalmol* 2006;50:85–89.
- Koh S, Maeda N, Hirohara Y, et al. Serial measurements of higher-order aberrations after blinking in normal subjects. *Invest Ophthalmol Vis Sci* 2006;47:3318–3324.
- Ninomiya S, Fujikado T, Kuroda T, et al. Changes of ocular aberration with accommodation. *Am J Ophthalmol* 2002;134:924–926.
- Cheng H, Barnett JK, Vilupuru AS, et al. A population study on changes in wave aberrations with accommodation. *J Vis* 2004;4:272–280.
- Zhu M, Collins MJ, Robert Iskander D. Microfluctuations of wavefront aberrations of the eye. *Ophthalmic Physiol Opt* 2004;24:562–571.
- Nemeth J, Erdelyi B, Csakany B, et al. High-speed videotopographic measurement of tear film build-up time. *Invest Ophthalmol Vis Sci* 2002;43:1783–1790.
- Goto T, Zheng X, Klyce SD, et al. A new method for tear film stability analysis using videokeratography. *Am J Ophthalmol* 2003;135:607–612.

13. Kojima T, Ishida R, Dogru M, et al. A new noninvasive tear stability analysis system for the assessment of dry eyes. *Invest Ophthalmol Vis Sci* 2004;45:1369–1374.
14. Montes-Mico R, Alio JL, Charman WN. Dynamic changes in the tear film in dry eyes. *Invest Ophthalmol Vis Sci* 2005;46:1615–1619.
15. Tutt R, Bradley A, Begley C, Thibos LN. Optical and visual impact of tear break-up in human eyes. *Invest Ophthalmol Vis Sci* 2000;41:4117–4123.
16. Born M, Wolf E. Principles of optics: electromagnetic theory of propagation, interference and diffraction of light, 7th expanded ed. New York: Cambridge University Press; 1999. p. 417–446, 518–520.
17. Howland HC. High order wave aberration of eyes. *Ophthalmic Physiol Opt* 2002;22:434–439.
18. Born M, Wolf E. Principles of optics: electromagnetic theory of propagation, interference and diffraction of light, 7th expanded ed. New York: Cambridge University Press; 1999. p. 522.
19. Applegate RA. Glenn Fry award lecture 2002: wavefront sensing, ideal corrections, and visual performance. *Optom Vis Sci* 2004;81:167–177.
20. Oshika T, Mimura T, Tanaka S, et al. Apparent accommodation and corneal wavefront aberration in pseudophakic eyes. *Invest Ophthalmol Vis Sci* 2002;43:2882–2886.
21. Cheng X, Bradley A, Thibos LN. Predicting subjective judgment of best focus with objective image quality metrics. *J Vis* 2004;4:310–321.
22. Tsubota K, Hata S, Okusawa Y, Egami F, Ohtsuki T, Nakamori K. Quantitative videographic analysis of blinking in normal subjects and patients with dry eye. *Arch Ophthalmol* 1996;114:715–720.
23. Ridder WH, 3rd, Tomlinson A. Suppression of contrast sensitivity during eyelid blinks. *Vision Res* 1993;33:1795–1802.
24. Vongthongsri A, Phusitphoykai N, Nariphapan P. Comparison of wavefront-guided customized ablation vs. conventional ablation in laser in situ keratomileusis. *J Refract Surg* 2002;18:S332–335.
25. Kim TI, Yang SJ, Tchah H. Bilateral comparison of wavefront-guided versus conventional laser in situ keratomileusis with Bausch and Lomb Zyoptix. *J Refract Surg* 2004;20:432–438.
26. Nagy ZZ, Palagyi-Deak I, Kelemen E, Kovacs A. Wavefront-guided photorefractive keratectomy for myopia and myopic astigmatism. *J Refract Surg* 2002;18:S615–619.
27. Panagopoulou SI, Pallikaris IG. Wavefront customized ablations with the WASCA Asclepion workstation. *J Refract Surg* 2001;17:S608–612.
28. Thai LC, Tomlinson A, Ridder WH. Contact lens drying and visual performance: the vision cycle with contact lenses. *Optom Vis Sci* 2002;79:381–388.
29. Ishida R, Kojima T, Dogru M, et al. The application of a new continuous functional visual acuity measurement system in dry eye syndromes. *Am J Ophthalmol* 2005;139:253–258.